A Detailed Characterization of Spectral Regridding for the WSU Era

Sean M. Andrews[1], Ryan A. Loomis[2], Chunhua Qi[1], Jennifer Donovan Meyer[2], Todd R. Hunter[2], Andrew Lipnicky[2], and Garrett K. Keating[1]

[1] — Center for Astrophysics | Harvard & Smithsonian, 60 Garden Street, Cambridge, MA, USA 02138
[2] — National Radio Astronomy Observatory, 520 Edgemont Road, Charlottesville, VA 22903

Executive Summary:

We analyzed various approaches for spectral regridding of simulated data in both the noise- and signal-dominated regimes to assess the behaviors of the current ALMA baseline correlator (BLC) and the forthcoming Wideband Sensitivity Upgrade (WSU). We find that:

- there are real risks to maintaining the current default spectral regridding approach for WSU data, but they can be mitigated with some straightforward software adjustments;
- there are substantial benefits, and only minimal disadvantages, to switching the default interpolation algorithm in the spectral regridding from `linear` to `fftshift`;
- the order of operations in offline spectral regridding should default to performing spectral averaging *after* frame transformation and interpolation (avoiding pre-averaging).

1. Motivation and Background

For most ALMA users, spectral signal processing receives much less attention than, for example, efforts to optimize calibration or imaging. However, these are not unrelated issues. As ALMA prepares to transition their instrumentation to realize the Wideband Sensitivity Upgrade (WSU), along with an accompanying software refactoring and expansion in the user-facing archive (with more advanced science-ready data products), it is an opportune time to consider how various aspects of spectral processing contribute to the overall quality of the data products.

This ALMA Development Study focuses on assessing the advantages and shortcomings of various approaches for that spectral processing, both now and in the future with the WSU. Our approach was based on a suite of retrieval analyses, where known signals were injected into realistic simulations of data, processed in some way, and then compared to the inputs to assess the quality of the recovered signal. This section offers some background, to ground the discussion of the simulations (§2) and analyses (§3–4) that inform our conclusions (§5) and drive our recommendations (§6).

1.1. Spectral Signal Processing in Digital Correlators

For each discrete measurement from some pair of antennas (indexed $\mathtt{ij}$), the ALMA correlator measures the complex visibility as a function of frequency $\mathcal{V}_{\mathtt{ij}}(\nu)$. This is a cross-power spectrum, the Fourier transform of the cross-correlation of voltage timestreams $V(t)$ from each antenna weighted by a digital filter, or 'windowing' function $W(\tau)$,

$$\mathcal{V}_{\mathtt{ij}}(\nu) = \boldsymbol{\mathcal{F}}_{\nu}\{W(\tau) \cdot \langle V_{\mathtt{i}}(t) * V_{\mathtt{j}}(t) \rangle\}, \tag{1}$$

where $\boldsymbol{\mathcal{F}}_{\nu}\{\,\}$ denotes the Fourier transform from the time to the frequency domain and τ represents the lag that controls the sampling rate of the timestreams. We can use the Fourier convolution

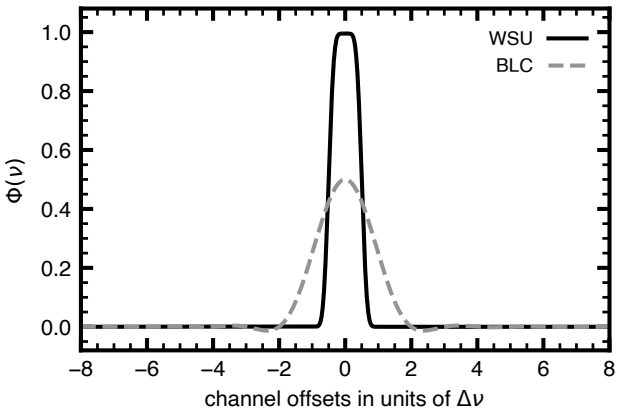

Figure 1: Comparison of the spectral response functions $\Phi(\nu)$ for the baseline correlator (BLC) and the ATAC correlator to be deployed for the WSU, in units of the native channel spacing $\Delta\nu$ (and properly normalized to conserve power). With the WSU, the FWHM of $\Phi(\nu)$ is $\sim\Delta\nu$, compared to $2\Delta\nu$ for the BLC. The WSU channels will be significantly less correlated, and less power will be distributed in high-frequency sidelobes.

theorem to instead rewrite Eq. (1) as

$$\mathcal{V}_{\mathtt{ij}}(\nu) = \underbrace{\boldsymbol{\mathcal{F}}_\nu\{W(\tau)\}}_{\Phi(\nu)} * \underbrace{\boldsymbol{\mathcal{F}}_\nu\{\langle V_{\mathtt{i}}(t) * V_{\mathtt{j}}(t)\rangle\}}_{\widetilde{\mathcal{V}}_{\mathtt{ij}}(\nu)}. \tag{2}$$

The specific form of Eq. (2) makes it clearer that the output ("observed") visibility spectrum from the correlator is the convolution of the "true" visibility spectrum from the source $\widetilde{\mathcal{V}}_{\mathtt{ij}}(\nu)$ and a *spectral response function* $\Phi(\nu)$, which is itself the Fourier transform of the windowing function.[1] In practice, the correlator samples voltage streams at discrete time (lag) intervals τ, which determine the frequency sampling rate as the *native* channel spacing $\Delta\nu \sim 1/\tau$.

The spectral response function defines the spectral resolution, corresponding to its main lobe FWHM in units of the native spacing. Figure 1 shows $\Phi(\nu)$ for the current ALMA baseline correlator (BLC) and the expectations for the ATAC correlator that will replace it during the WSU. The WSU will see a factor of two improvement in resolution (relative to $\Delta\nu$), offering spectral channels that are effectively independent. This mitigation of the spectral covariance plays important roles in various outcomes of the spectral signal processing, as we will demonstrate below.

1.2. Doppler Setting and the Need for Spectral Regridding

The ALMA correlators (now and with the WSU) process and record data in the topocentric (`TOPO`) reference frame, using a frequency channel grid that is fixed at the start of each execution block (*Doppler setting*). Each subsequent integration is therefore sampling the source spectrum at a *different* set of frequencies in an inertial reference frame (e.g., `LSRK`) onto those `TOPO` channels. The connection between the fixed `TOPO` channels and the changing frequencies in the inertial (hereafter `LSRK`, although there are other options) frame is deterministic: it can be computed based on the relative motion of the source and observatory (using the source coordinates, observatory location, date, and time). When reconstructing images, or analyzing the data more generally, users need to consider their data in an inertial (source-oriented) reference frame like `LSRK`. This requires some post-processing referred to as *regridding*, a blanket term comprising three distinct processes:

- reference frame transformation (mapping channel frequencies from `TOPO` → `LSRK`);
- interpolation onto a fixed channel grid in the inertial (`LSRK`) frame; and
- averaging to an arbitrarily larger effective channel spacing (if desired).

[1] This is colloquially referred to as *Hanning smoothing*, though that is confusing nomenclature.

Most of the inaccuracies introduced by spectral regridding are related to the chosen spectral interpolation algorithm and the order of operations for executing these three processes.

1.3. Default Regridding

Aspects of the spectral regridding process can be performed *online* – within the correlator, before the data are recorded – or *offline*, using common tasks in the CASA software package (e.g., mstransform, cvel2, tclean). The default for current ALMA operations includes an online *pre-averaging* (bin $\times 2$ native channels), although for some science cases users may request to receive data with the native `TOPO` spacing. For offline regridding with CASA, users specify an output channel spacing $\Delta\nu_{\texttt{out}}$, starting frequency, number of channels, and output reference frame. When $\Delta\nu_{\texttt{out}} > 2\Delta\nu$, these CASA tasks pre-average (in the `TOPO` frame), transform frames, and then interpolate to the specified channels in the output frame. Otherwise (when $\Delta\nu_{\texttt{out}} \leq 2\Delta\nu$), the pre-averaging step is skipped. The default for all regridding tasks in CASA, and the ALMA operations pipelines built on CASA tasks, is to adopt a simple `linear` interpolation algorithm (Hunter et al. 2023).

The default order of operations in current practice – particularly pre-averaging before the frame transformation and interpolation – is not ideal, since it correlates the data in the spectral dimension in a non-trivial and irreversible way. The motivation is practical: online pre-averaging reduces the data rate, and offline pre-averaging minimizes the computational costs for the subsequent transformation and interpolation steps in the regridding process (then further data reduction). We will explore the effects of this default pre-averaging in the regridding process in §4.1.

2. Simulations

Our goal is to explore the quality of various regridding approaches along several performance axes. In particular, we will consider their behaviors in the noise- and signal-dominated regimes. For the latter, we generated some realistic synthetic observations as described in the following subsections.

2.1. Emulating ALMA Spectral Signal Processing

We simulated a set of ALMA molecular line observations as a guide for this study. The underlying emission model is representative of the ^{12}CO J=2−1 (rest frequency 230.538 GHz; Band 6) emission from a protoplanetary disk. Disks are an especially useful test case for this study, since much effort in the field is focused on characterizing subtle spectral features that can be affected by the regridding process (e.g., the Large Programs MAPS [2018.1.01055.L] and exoALMA [2021.1.01123.L]). More generally, analogous science cases across many sub-disciplines advocating for high fidelity, high spectral resolution imaging serve as key science drivers for the WSU (Carpenter et al. 2022).

We defined an observational template, specifying a set of (u, v) spatial frequency coordinates for a given observing configuration at a given date and time, along with a fixed grid of native channels (with spacing $\Delta\nu$) in the `TOPO` frame. For each timestamp in the template, we generated a model line intensity cube on the `LSRK` frequencies that correspond to these fixed `TOPO` channels,[2] and computed a spatial Fourier-transform of each spectral plane sampled onto the appropriate (u, v) points. Following Equation (2), this resulting set of "true"/input visibility spectra, $\widetilde{\mathcal{V}}(\nu)$, was then convolved with the appropriate spectral response function, $\Phi(\nu)$, to give the "observed"/output

[2] In practice, we over-sampled these frequency channels by a factor of 10, then decimated by that factor after the convolution by the spectral response function.

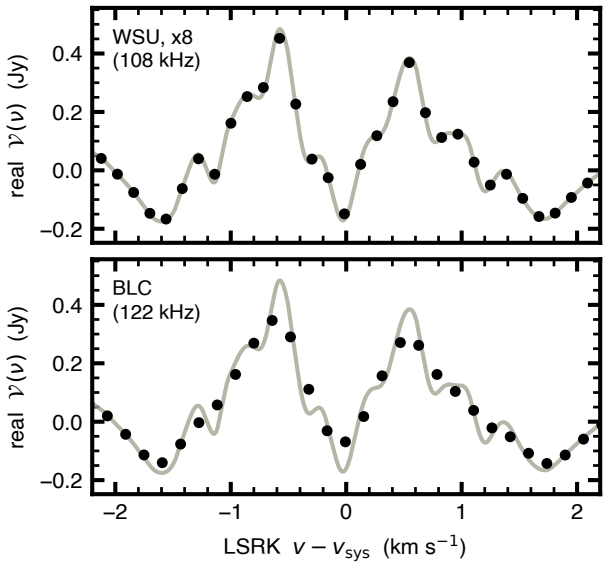

Figure 2: Representative observed visibility spectra (real parts) from a disk model (at a u, v-distance of 250 kλ). The true input spectrum (sampled at 1 kHz) is a gray curve. The black points are the true spectrum convolved with the spectral response function and sampled at the native channel spacing: in the top panel for the WSU, these were then binned by 8 native channels to emulate online pre-averaging. The observed WSU data are a *much* better match to the truth than the BLC data (even with the binning) because the spectral response function for the latter is $\sim$18$\times$ ($2 \times 122/13.5$) broader.

visibility spectra, $\mathcal{V}(\nu)$. These simulations were conducted with the csalt package[3], which in this use case invokes the both the CASA.simobserve task and the vis_sample package[4].

2.2. Reference Simulations

The underlying source model was a Keplerian protoplanetary disk orbiting a Sun-like star at a projected viewing angle (inclination) of 30° (where 0° is face-on), designed to be representative of a typical target in a nearby star-forming region (in terms of size and flux). We defined the observational template to emulate brief (15 minutes on-target) measurements in the C–6 configuration on April 20, 2025, for a target at R.A.=16$^{\rm h}$, Decl.=−30°, and starting at HA=0$^{\rm h}$. We explored simulations with a variety of correlator configurations for this study, but ultimately will present the results from two representative configurations: a BLC configuration with native spacing $\Delta\nu = 122$ kHz ($\sim$160 m s^{-1}) and a WSU configuration with online pre-averaging (binning the 13.5 kHz native spacing by a factor of 8) to an effective $\Delta\nu = 108$ kHz ($\sim$140 m s^{-1}). Both configurations are designed to sample the model emission with the common velocity resolution expected for most studies of protoplanetary disks (i.e., roughly Nyquist-sampling the characteristic linewidths).

For the analysis (§3), a benchmark is useful for the regridding comparisons. For that purpose, we generated a very fine-sampled (1 kHz) version of the models to represent the ***true*** input visibility spectra. These were convolved with the relevant spectral response function and then interpolated (the 1 kHz sampling is suitably high that interpolation inaccuracies can be neglected) and *post*-averaged (binned) when appropriate to serve as ***reference*** visibility spectra to be compared with the regridded data products. By comparison, the ***observed*** spectra were defined by convolving the true input spectra with the spectral response function and downsampling to the native channel spacing ($\Delta\nu$); for the WSU, those downsampled spectra were then binning by 8 native (13.5 kHz) channels to emulate online pre-averaging to an effective $\Delta\nu = 108$ kHz. We refer to the ***interpolated*** data as the products of applying some interpolation algorithm to those observed spectra that shifts them by some fraction of the channel spacing. Figure 2 illustrates the effects of the simulated spectral signal processing on representative visibility spectra for the BLC and WSU.

[3] https://github.com/seanandrews/csalt/
[4] https://github.com/AstroChem/vis_sample

For visualization purposes, we sometimes compared these simulations in the image domain (i.e., channel maps). To avoid any complications induced by deconvolution, this was typically done using the dirty images generated by CASA.tclean assuming natural weighting (without regridding during the imaging process, by setting `specmode=cubedata`).

3. Regridding Analysis

We considered two key concepts that define an optimal regridding method:

1. ***variance preservation***, meaning the statistical properties of the noise are not changed; and
2. ***signal fidelity***, meaning the quality of the spectral signal is minimally corrupted.

In practice, these can be characterized by considering the behaviors of regridding approaches in the noise-limited (low SNR) and signal-limited (high SNR) regimes. Of course, no regridding approach is perfect in both regimes; some perform much better in one or the other. Our aim was to characterize the performances of different approaches for both of these metrics.

As noted above, the regridding process includes a reference frame transformation (which is *analytic*), an interpolation, and (if requested) an averaging. We restricted ourselves to considering online averaging only for the WSU case (i.e., not the BLC case). For now, we also put aside the order of operations in order to focus here on the action of the interpolation algorithm. We comment on offline averaging and the order of operations in §4.1.

3.1. Interpolation Algorithms

The available CASA spectral interpolation options are nearest-neighbor (`nearest`), linear (`linear`; set as the default), and cubic spline (`cubic`) interpolation. The key advantages of these algorithms are their speed and simplicity: all of them are non-parametric methods. That said, these algorithms have some undesirable properties (see below), so we surveyed a variety of alternatives designed to achieve similar goals (Lepot et al. 2017 provides a nice overview of options). These included some traditional digital signal processing approaches – Fourier interpolation, Lanczos kernels (e.g., Burger & Burge 2009), radial basis functions (Franke 1982), prolate spheroidal functions (Slepian 1978), wavelet transforms (Chui 1992) – as well as more sophisticated stochastic methods developed for machine learning applications – various auto-regressive approaches (e.g., Oudre 2018) or Gaussian processes (Williams 1998). However, it quickly became apparent that any potential benefits for most of these options are outweighed by considerable disadvantages in terms of compute speed and/or complexity (e.g., tuning parameters that depend a lot on the detailed use case).

Ultimately, our focus settled on variants of the classical Fourier interpolation methods. We will highlight and advocate specifically for the `fftshift` algorithm (also non-parametric), which as the name suggests can adequately recover a band-limited signal using a phase shift of the spectrum's Fourier transform. While there is a *latent* option for `fftshift` in the various CASA tasks that perform regridding (presumably inherited from AIPS^{++}, where it was the default), the code has a bug associated with packing the Fourier frequencies that renders the output incorrect (see §5).

3.2. Noise-Limited Regime

In the noise-limited (i.e., low SNR) regime, some spectral interpolation algorithms can modify the noise by increasing the covariance beyond what is already introduced by the spectral response function (i.e., power leaks from on-diagonal to off-diagonal terms in the covariance matrix; Loomis

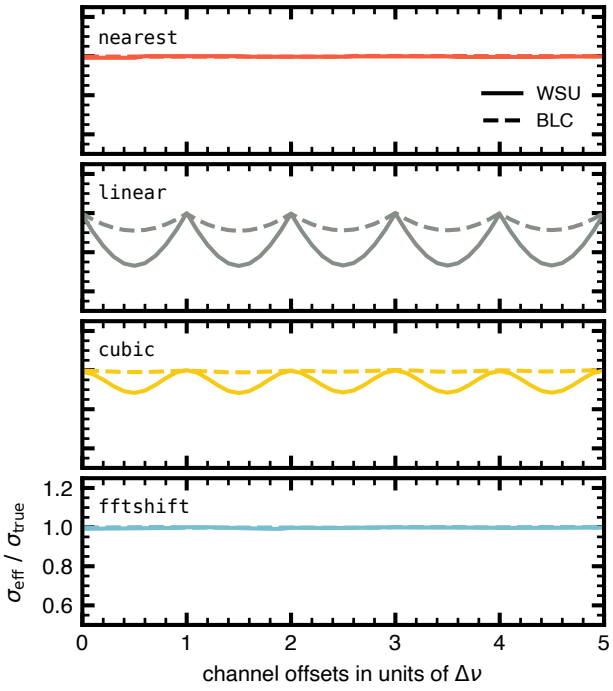

Figure 3: A demonstration of the effects that spectral interpolation has on noise in ALMA observations. Random noise spectra (drawn from a Gaussian process with variance $\sigma^2_{\rm true}$) are convolved with the spectral response function for the BLC or WSU and interpolated onto channels with shifts of various fractions of the native spacing ($\Delta\nu$). The effective variance over the draws in each interpolated offset channel is compared relative to the inputs. The `linear` and `cubic` algorithms introduce a 'scalloping', where the effective noise is artificially diminished. Those effects are more important for the quasi-independent channels of the WSU. However, the `nearest` and `fftshift` algorithms preserve the input variance.

et al. 2018). The net impact is that the measured, *effective* RMS noise of the regridded data appears artificially lower than the true noise (as injected or measured from the native data without regridding). Leroy et al. (2021) offered a particularly clear exposition of this effect based on examinations of the extensive ALMA datasets for the PHANGS Large Program [2017.1.00886.L]. Figure 3 revisits their approach, with some appropriate modifications. To quantify these effects for different interpolation algorithms, we generated a large number (10^5) of random noise spectra (oversampling the native spacing $\Delta\nu$ by a factor of 10), convolved these with the appropriate spectral response function, and then decimated back to the native spacing. We then interpolated each of those spectra onto a set of interpolated channels with sub-channel offsets (every $0.1\Delta\nu$) for a given algorithm. At each offset, we computed the standard deviation of the draws as $\sigma_{\rm eff}$.

Both the `nearest` and `fftshift` interpolation algorithms preserve the statistical noise properties of the input data, with essentially identical performance (regardless of $\Phi(\nu)$). This is not the case for `linear` or `cubic` interpolation, because these algorithms use neighboring points and therefore effectively smooth over more channels (the `cubic` case uses more neighbors, and so has a muted impact). For the quasi-independent native channels with the WSU, `linear` interpolation can reduce the variance by a factor of two ($\sigma_{\rm eff} \approx \sqrt{2}\sigma_{\rm true}$) for interpolates midway between native channels (the effect is less pronounced for the BLC because of the broader spectral response function).

In a sense, these effects are modest (particularly for the BLC). However, the more significant effects for the WSU mean that, moving forward, a robust accounting of the noise is essential for assessing quality and properly quantifying measurements, not to mention overall scientific accuracy. There is good motivation to adopt an interpolation algorithm that preserves variance.

3.3. Signal-Limited Regime

The signal-limited (i.e., high SNR) regime encapsulates a more expansive parameter space to explore. However, even restricting to some limited illustrative examples is sufficient to generalize the issues associated with regridding. Figure 4 illustrates the effects of the different interpolation

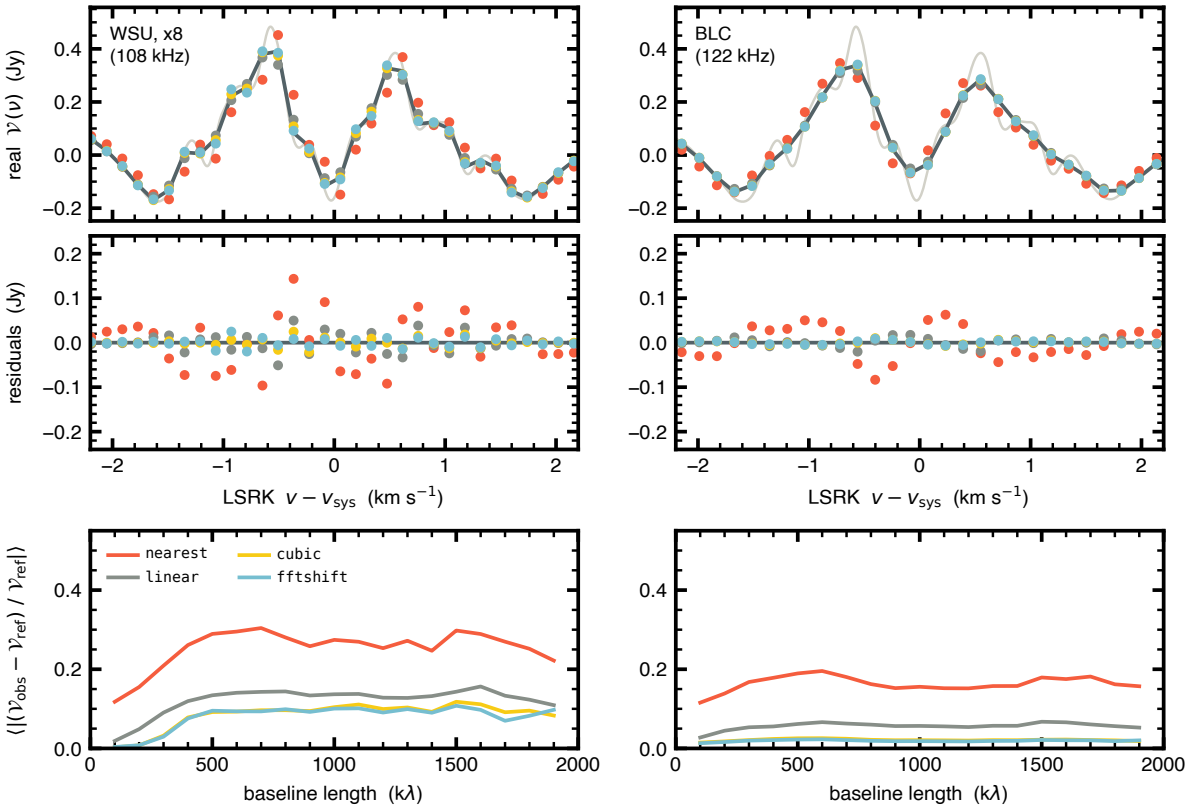

Figure 4: (*top*) A representative visibility spectrum (real parts; as in Fig. 2) interpolated to a $0.4\Delta\nu$ interval with four different algorithms, for simulations of the pre-averaged WSU at an effective spacing of 108 kHz (*left* column) and the BLC at a native spacing of 122 kHz (*right* column). Light gray curves show the true input spectrum, and dark gray curves show the reference spectrum (convolved with $\Phi(\nu)$ and averaged as appropriate). (*middle*) The residuals of the interpolated spectra compared to the reference. (*bottom*) The median fractional deviations of the residuals (including real and imaginary components) over the same spectral range in the middle panels as a function of the baseline length (for reference, the examples in the top and middle panels have a baseline length of 250 kλ).

algorithms for a segment of a single visibility spectrum (real parts only; at a spatial frequency distance of 250 kλ) in the (pre-averaged) WSU and BLC simulations. We assessed the signal fidelity, loosely defined here as the difference between the *regridded* (colored points) and *reference* (dark curves) spectra, in this example for the interpolation scenario of a 0.4-channel shift. In the bottom row panels, we show the median (absolute, including both real and imaginary components) *fractional* deviations for this spectral range as a function of the baseline length (note that at shorter baselines, the absolute deviations are larger even though they are fractionally smaller). For both correlator configurations, the relative signal fidelity using `nearest` is poor (as would be expected). The default `linear` shows slightly improved results, but performs considerably worse than `cubic` or `fftshift`, which have overall similar fidelity averaged over the full dataset.

In general, the degraded signal fidelity that results from interpolation is more apparent for the (online pre-averaged) WSU compared to the BLC. The underlying reason is the same as was demonstrated in the noise-limited regime: the intrinsic spectral variations are reduced (the signals in different channels are more correlated) for the broader spectral response function of the BLC, so

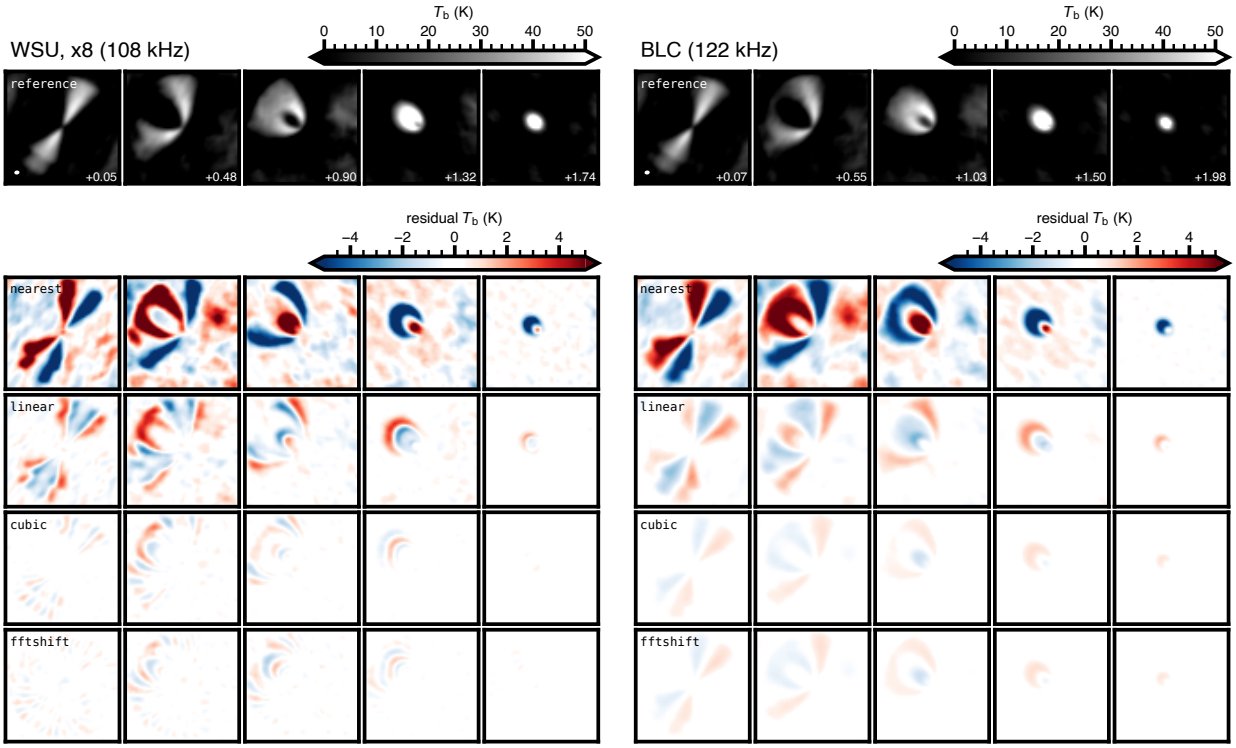

Figure 5: (*top*) Naturally-weighted, dirty channel maps at the effective channel spacings for the reference simulations (shifted by $0.4\Delta\nu$) for the (online, pre-averaged) WSU (*left columns*) and BLC (*right columns*) simulations, on a linear brightness temperature scale. The bottom right corners of each panel mark the LSRK velocities (in km/s); the bottom left corners of the first panels show the dirty beam dimensions. (*bottom rows*) The residual channel maps (interpolated − reference) for different algorithms. In this example, the `nearest` and `linear` algorithms perform with similarly poor quality; the `cubic` and `fftshift` algorithms are comparable and offer substantial improvements.

interpolation 'residuals' as defined here are correspondingly smaller. Analogously, the fidelity under interpolation depends on the intrinsic scale of spectral variations with respect to the effective channel spacing. Stronger spectral gradients at or below the channel spacing diminish the interpolation performance for all algorithms, and vice versa. For example, we see considerable improvements for simulations of the same underlying model that adopt finer native channel spacings (e.g., 61 kHz for the BLC or $\times 4$ pre-averaging for the WSU).

That said, our definition of *fidelity* is subtle, but important. It was entirely driven by the narrowly focused exploration of regridding, in isolation from other signal processing effects: the reference we chose is meant to represent what would be observed if no interpolation were required. On an absolute scale, if we instead referenced to the true input spectrum, the quality of the comparisons between the WSU and BLC are reversed. In that case, the quasi-independent native WSU channels ensure that the observed (and interpolated) spectra are generally much better representations of the input signal from the source. Though we want to keep the focus on the regridding effects on the data (as processed in the correlators), this distinction is worth highlighting (see the Appendix).

Figure 5 illustrates these same effects in the image domain, using a subset of dirty channel maps from the results shown in Figure 4. We find the same behaviors are manifested in the residual channel maps (the image-domain differences between the interpolated and reference channel maps):

stronger residuals are present for the `nearest` and `linear` algorithms, and more generally for the (pre-averaged) WSU simulations compared to the BLC. Overall, the residuals for the default `linear` interpolation algorithm can average ∼5–10% over many independent beams in these examples. That behavior can be suppressed by a factor of $\gtrsim 3$ simply by choosing a different algorithm.

4. Other Considerations

4.1. Regridding Order of Operations

The analysis presented so far presumes the 'standard' order of operations for regridding, generally applicable when (online) pre-averaging is performed. We suggested in §1.3 that this order is sub-optimal. Ideally, the regridding process would perform frame transformation, interpolation, and then (offline) *post*-averaging if desired. The motivations for online averaging are practical constraints: reducing data rates and post-processing (calibration) computing costs. However, for *offline* spectral processing, this 'short-cut' offers no real benefit for the data rates, and the computing costs seem insignificant compared to the deleterious effects of pre-averaging.

When the amount of averaging is small, the demonstrated effects of the interpolation operation will dominate. When the number of channels being averaged to the final output channel is high, however, the order of operations for this averaging will begin to play a larger role. Both of these scenarios will certainly arise in WSU operations and in re-imaging of archival WSU data. Figure 6 illustrates the comparative cost of offline averaging with the standard and suggested order of operations, using the ×8 binning for the WSU simulations (108 kHz channels). As shown before (in Fig. 5), the pre-averaging imposes significant artifacts under the interpolation operation. While these are mitigated fairly well by adopting the `cubic` or `fftshift` algorithms, the residuals remain relatively high. However, if the data rate is not an issue, we demonstrate that switching the order of operations to perform the interpolation first (i.e., *post*-averaging) essentially eliminates these artifacts. The residuals are negligible and effectively the same for all interpolation algorithms: these are simply the manifestations of the binning operation, since the interpolation happens at the native (13.5 kHz) spacing, which significantly oversamples the intrinsic model variations.[5] In a framework where regridding is only performed once by the typical user, there is not a compelling justification to maintain the current CASA standard for the order of operations for offline regridding.

4.2. A Demonstration with Real Data

We have been illustrating the salient issues with spectral regridding using controlled experiments, injecting known input signals into realistic simulations and comparing the outputs to those references. However, we do think it is relevant to demonstrate that these issues are indeed present in real ALMA data. Though we do not know the true input spectra from an astronomical source as a reference, we can compare outputs from different interpolation algorithms relative to one other.

Figure 7 is an example of this type of relative comparison, using observations of the ^{12}CO J=2−1 line emission from the HD 163296 protoplanetary disk taken for the MAPS Large Program (Öberg et al. 2021). Here, we adopted a similar regridding procedure as was used for the MAPS data delivery – performing an offline pre-averaging over two native (61 kHz) channels (with corresponding output channel spacing ∼160 m s^{-1}) – and then interpolating again by a half-channel shift. The

[5]Obviously this is a dramatic illustration. Even for a typical protoplanetary disk, the WSU native channel spacing can produce more significant regridding artifacts for post-averaged data when the intrinsic spectral variations are relatively larger (e.g., for Band 1 or 2 emission lines).

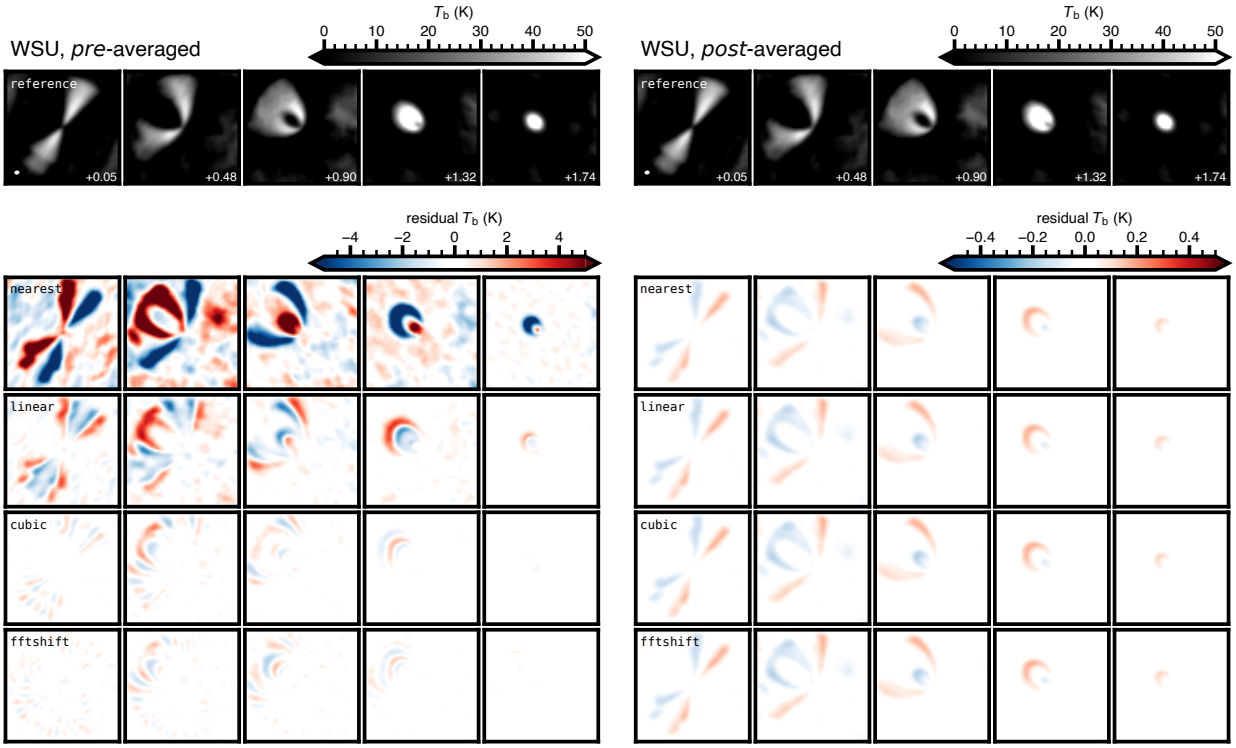

Figure 6: The same formatting as in Fig. 5, but here comparing the interpolation residuals between the pre-averaged (*left*; identical to Fig. 5) and post-averaged (*right*) WSU data. **Note the factor of 10 difference between the residual colorscales in this comparison.** Clearly, if spectral averaging is performed as part of the offline regridding process, there are significant advantages to changing the default order of operations and averaging after frame transformation and interpolation. The lingering low-level residuals in the right column are solely related to the binning process, since the interpolation happens on the WSU native channels that considerably oversample the spectral variations of the model.

naturally-weighted, dirty channel map residuals are shown with respect to the `fftshift` case. Just as for the simulations, we find in this real data example that `cubic` and `fftshift` provide very similar outputs, with much more substantial differences when comparing to the `linear` or `nearest` algorithms. For context, this comparison demonstrates that the choice of interpolation algorithm can produce artifacts $\sim$1–2$\times$ the RMS noise over many independent beams in each output channel. Such artifacts can have significant downstream impacts on the science: in this case, there is risk to mis-diagnosing the gas dynamics, particularly the detailed disk velocity field (e.g., Andrews et al. 2024) and line broadening from microturbulence (e.g., Flaherty et al. 2020).

4.3. Some Practical Concerns with `fftshift`

While the preceding analysis makes a strong case that the `fftshift` interpolation algorithm is a desirable alternative for spectral regridding, it is of course not perfect. Here we address a few practical aspects of `fftshift` interpolation that merit explicit consideration if ALMA proceeds with integrating this option into the capabilities of CASA and its successor software.

First, we explored the expectations for the compute "cost" of different interpolation algorithms. There are several axes on which this cost could be defined, but we assumed that time (per visibility)

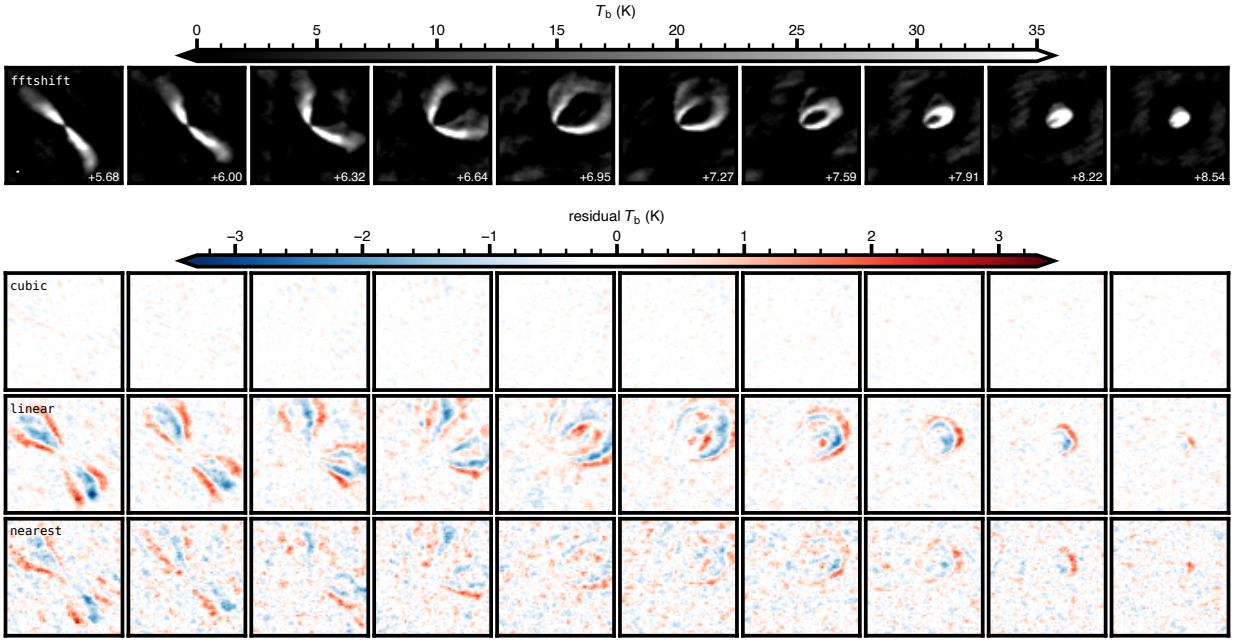

Figure 7: An inter-comparison of interpolation algorithms (here referenced to `fftshift`) for real CO J=2−1 observations of the HD 163296 protoplanetary disks from the MAPS program. The format and annotations are as in Figures 5 and 6. The RMS scatter in each set of channel maps is ∼1 K., so the differences between the interpolation algorithms can amount to ∼1–2σ over many independent beams.

per number of channels in the spectrum would be the most informative metric for those working on designing the WSU regridding infrastructure. Figure 8 compares the interpolation algorithms considered here in this context. For the $\sim 8 \times 10^4$ channels in a full WSU spectral window, the cost of switching from `linear` to `fftshift` as the default interpolation algorithm is only ∼25%.[6] While recommendations of software design strategies are beyond the scope of our efforts, these behaviors should give a reasonable estimate of the tradeoffs between parallelizing along the spectral axis or

[6]This presumes adopting an efficient `FFT` package. Here we are using the default `LAPACK` setup inside `numpy`, which suffers a factor of a few hit (comparable to the `cubic` curve) for spectra with channel numbers that are not a power of two. While this can be mitigated with zero-padding, it can instead be solved and even improved with available open-source alternatives (e.g., `FFTW`).

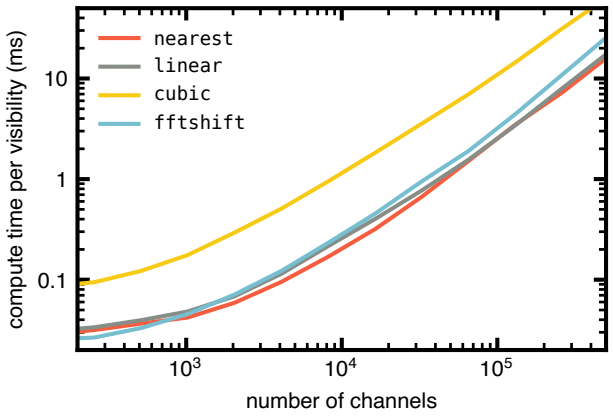

Figure 8: Simple estimates of the mean (over 1,000 trials per point) compute time for interpolating a single visibility spectrum with a given number of channels for the different algorithms considered here. The normalization is presumably CPU architecture-dependent, but relative differences should still be appropriate. With an optimized `FFT` package, `fftshift` does not incur an onerous cost compared to the default.

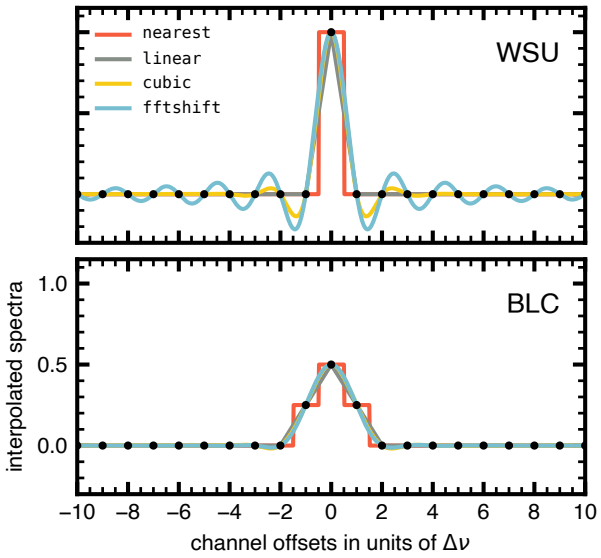

Figure 9: The responses of the different algorithms to interpolating a sharp impulse feature introduced before the windowing operation in the correlator (the input spectrum in black points) for (*top*) the WSU and (*bottom*) BLC. Because the WSU native channels are nearly independent, the top panel is a reasonably good representation of the behavior when such an artifact is introduced after the windowing operation (even for the BLC). For quasi-independent channels, the `cubic` and `fftshift` algorithms can introduce spurious oscillations. Some form of artifact removal process would be required to mitigate any such lingering features.

some other domain (e.g., splitting a WSU window into chunks is only a modest savings in compute time, and there are then complexity costs associated with re-stitching the outputs together).

One downside associated with some interpolation algorithms is that strong features varying faster than the native sampling rate can introduce artifacts. Given the canonical oscillatory behavior expected from Fourier transforms of sharp features, it is not surprising that the `fftshift` algorithm suffers from this problem. In practice, this is usually a design decision for the observations and target: it is obviously best to select an effective channel spacing that oversamples the intrinsic spectral variations. But in some cases this cannot be known a priori or achieved in practice (e.g., masers). Or, there can be artifacts ('spikes') contributed by RFI, the atmosphere, or instrument. Figure 9 illustrates the results of interpolating such an unresolved, sharp 'impulse' spectrum.

When such features are introduced before the windowing operation in the correlator, the broader spectral response function for the BLC mitigates the problem equally well for all the interpolation algorithms: the impact is minimal. But for the quasi-independent channels with the WSU (or where a spike is introduced after the windowing, even in the BLC), interpolation with the `cubic` and `fftshift` algorithms can introduce undesirable ringing artifacts. In those contexts, if such features are intrinsic to the source, damping out this ringing using spectral averaging is a desirable aspect of the regridding process. Some careful consideration will need to be given to cases where such features are RFI or instrument artifacts, since flagging or blanking channels can be problematic in the standard `cubic` or `fftshift` frameworks (e.g., perhaps some mitigation using a two-layered interpolation, deploying `nearest` or `linear` first for blanked channels).

One potential advantage of adopting `fftshift` for interpolation is that its performance does not noticeably degrade over multiple operations. This property is just a manifestation of the Fourier shift theorem. On the contrary, the spectral fidelity steadily degrades with each interpolation for both the `linear` and `cubic` algorithms (notably worse for `linear`). The results for `nearest` do not change monotonically, but as we showed above the mean result for even a single operation is poor. Although in general multiple regriddings may not be necessary, there may be scenarios in pipeline modes or offline reduction where this `fftshift` property will have some value for storing or reprocessing/staging data in the WSU era: there is no real loss of information if the data are regridded onto an LSRK grid with the native channel spacing.

5. Conclusions

Most analysis of ALMA spectral line data – and all imaging – requires regridding. But that process can degrade the signal quality and artificially modify the noise properties in ways that are difficult to track and essentially impossible to reverse. As ALMA users push the boundaries of the facility to probe new scientific areas enabled by spectral line data, it is crucial to minimize the quantitative impacts of regridding on those cutting-edge measurements. We anticipate these needs to grow in significance with the WSU. As we highlighted in this report, the quasi-independent channels from the ATAC correlator can amplify the regridding effects. Moreover, the improved sensitivity and flexibility of ALMA in the WSU era will spur more sophisticated science goals that rely on accurate representations of spectral line data. The development study described in this report explored how to minimize the influence of regridding on the interpretation of such data.

This report describes a representative subset of these explorations to illustrates some key concepts in a condensed format. These tradeoff studies considered various performance metrics of the regridding process, and were largely based on detailed simulated datasets that emulate the spectral signal processing in the ALMA baseline (BLC; current) and ATAC (WSU; forthcoming) correlators.

We can summarize the key findings from this study as:

- The impacts of regridding are minimized for channel spacings that oversample the characteristic spectral variations in the source. This is an obvious statement, but it serves to reinforce that design decisions for observations and default settings in the face of data rate limitations should be on the minds of both users and the Observatory: there is a potential scientific cost to online pre-averaging that needs to be considered in light of the specific science case.

- The order of operations with respect to averaging is an important factor in the fidelity of the output spectrum: *post*-averaging (after frame transformation and interpolation at the native channel spacing) always outperforms *pre*-averaging.

- The default `linear` interpolation in CASA regridding is the option with the poorest overall performance: it introduces the most (un-tracked) covariance, thereby artificially diminishing the effective noise, and does not deliver high-quality preservation of the source signal.

- The `fftshift` interpolation algorithm is an alternative option with overall excellent performance: it preserves both the noise properties and spectral fidelity of the input data with an effectively negligible practical (computational) cost and manageable cautionary 'edge cases' (e.g., some care is required for handling narrow artifacts).

We provide an open-source Python code repository that illustrates how the simulations and figures in this report were made, available at `https://github.com/seanandrews/ALMA_dev2023`.

6. Recommendations

In light of these findings, we recommend:

1. The offline facility software (CASA, and its descendants) team implements `fftshift` interpolation as an option for regridding, and transitions to setting it as the default for users. (For pipeline heuristics that rely on noise measurements as the key metric, `nearest` should be adopted as an appropriate immediate alternative to `linear`.) During this implementation and transition, it may make sense to adopt `cubic` interpolation as an interim default algorithm for offline regridding by users.
2. The offline facility software team implements a swap in the order of operations for regridding tasks, so that the default is *post*-averaging instead of the current *pre*-averaging.
3. Every reasonable effort should be made to enable early WSU users to obtain data at the native (13.5 kHz) spacing without online averaging when scientifically relevant.

Acknowledgments

We are especially grateful to Ian Czekala, for offering some important guidance and helpful code regarding `fftshift`; Thushara Gunaratne, for kindly providing a digital representation of the WSU spectral response function; and Rich Teague, for reviewing a draft version of this report. In exploring the results of our analysis, we also benefitted from several helpful conversations with Remy Indebetouw and Jan-Willem Steeb.

References

Andrews, S. M., et al. 2024, *Astrophysical Journal*, in press (arXiv:2405.19574)
Burger & Burge 2009, *Principles of Digital Image Processing: Core Algorithms*, Springer, 231
Carpenter, J. M., et al. 2022, *ALMA Memo 621*, arXiv:2211.00195
Chui, C. K. 1992, *An Introduction to Wavelets*, Academic Press, 177
Flaherty, K., et al. 2020, *Astrophysical Journal*, 895, 109
Franke, R. 1982, *Mathematics of Computation*, 38, 181
Hunter, T. R., et al. 2023, *Publications of the Astronomical Society of the Pacific*, 135, 4501
Lepot, M., Aubin, J.-B., & Clemens, F. H. L. R. 2017, *Water*, 9 (10), 796
Leroy, A. K., et al. 2021, *Astrophysical Journal Supplement Series*, 255, 1
Loomis, R. A., et al. 2018, *Astronomical Journal*, 155, 182
Öberg, K. I., et al. 2021, *Astrophysical Journal Supplement Series*, 257, 1
Oudre, L. 2018, *Image Processing On Line*, 23
Slepian, D. 1978, *Bell System Technical Journal*, 57, 1371
Williams, C. K. I. 1998, *Learning In Graphical Models*, 599

Appendix

As a point of clarity, we provide variants of Figures 4 and 5 that use the true input model spectra as the reference for illustrations of signal fidelity. These demonstrate that we expect the WSU to provide more accurate data in terms of the *absolute* spectral fidelity (with or without regridding) when the basis of comparison is the signal from the source to the telescope.

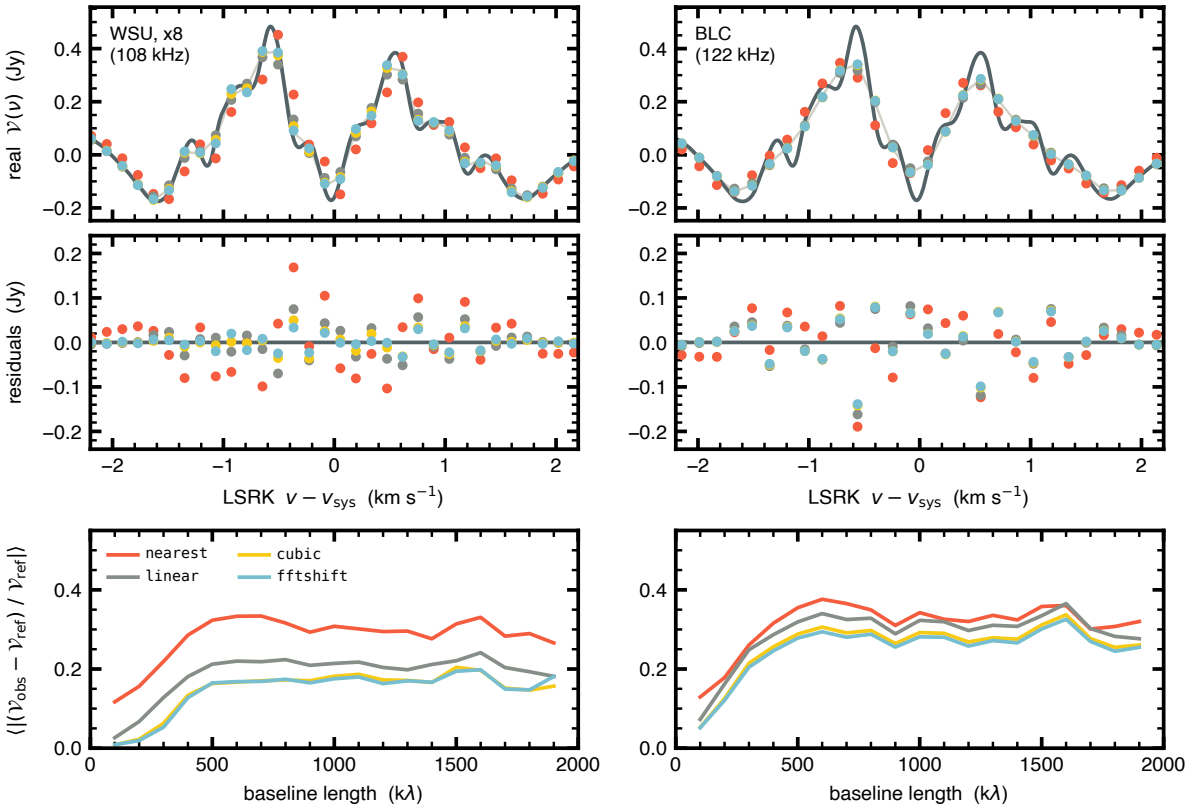

Figure 10: A modification of Figure 4, now showing the signal fidelity with the true source signal (no correlator processing) as the *reference* (dark gray curves in top panels). In comparing the figures, it is clear that the absolute fidelity for the WSU is significantly better than for the BLC, again owing primarily to the contribution of the narrower spectral response function.

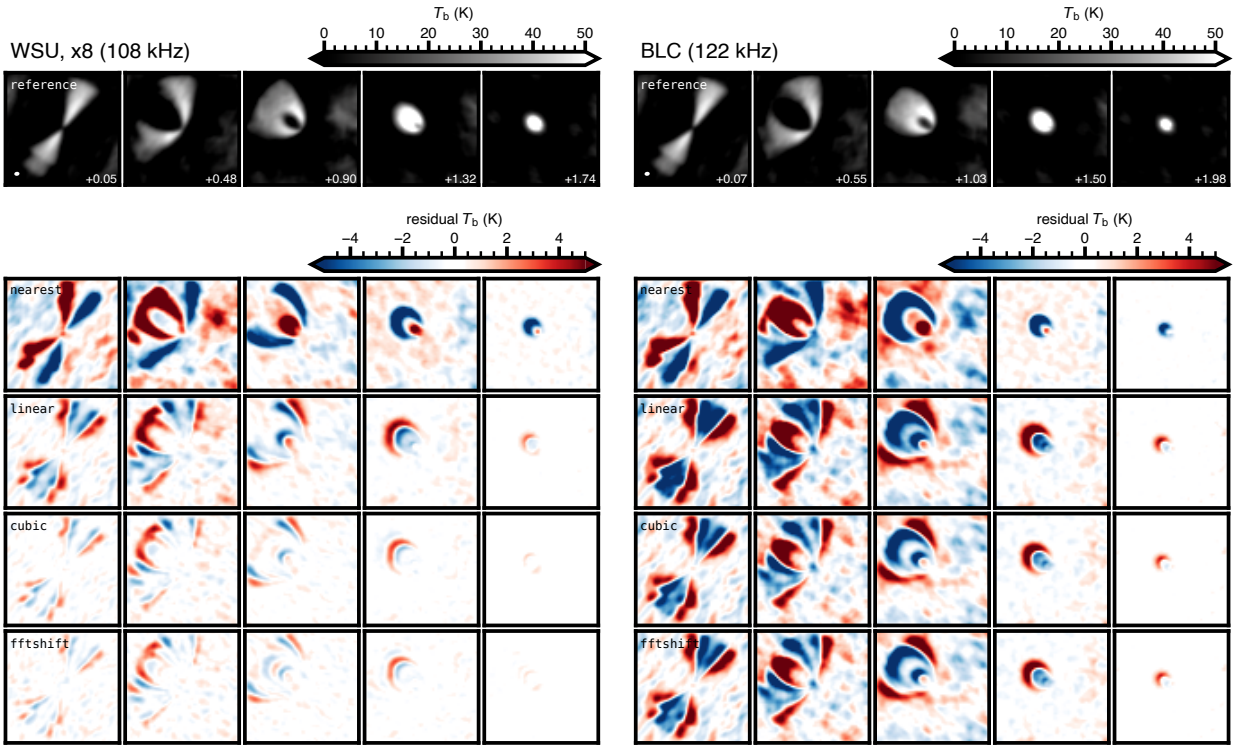

Figure 11: A modified version of Figure 5, now showing residuals with the true source signal (no correlator processing) as the *reference*. The WSU will provide a much better representation of the source spectra in an absolute sense, even with the inaccuracies introduced by regridding.